THE JOURNAL OF BIOLOGICAL CHEMISTRY VOL. 286, NO. 25, pp. 22478–22488, June 24, 2011


# 15-Lipoxygenase-1-enhanced Src-Janus Kinase 2-Signal Transducer and Activator of Transcription 3 Stimulation and Monocyte Chemoattractant Protein-1 Expression Require Redox-sensitive Activation of Epidermal Growth Factor Receptor in Vascular Wall Remodeling*

Received for publication, January 25, 2011, and in revised form, April 27, 2011 Published, JBC Papers in Press, May 2, 2011, DOI 10.1074/jbc.M111.225060

**Nikhlesh K. Singh, Dong Wang, Venkatesh Kundumani-Sridharan, Dong Van Quyen, Jixiao Niu, and Gadiparthi N. Rao**[1]

*From the Department of Physiology, The University of Tennessee Health Science Center, Memphis, Tennessee 38163*

**To understand the mechanisms by which 15(*S*)-hydroxyeicosatetraenoic acid (15(*S*)-HETE) activates signal transducer and activator of transcription 3 (STAT3), we studied the role of epidermal growth factor receptor (EGFR). 15(*S*)-HETE stimulated tyrosine phosphorylation of EGFR in a time-dependent manner in vascular smooth muscle cells (VSMCs). Interference with EGFR activation blocked 15(*S*)-HETE-induced Src and STAT3 tyrosine phosphorylation, monocyte chemoattractant protein-1 (MCP-1) expression and VSMC migration. 15(*S*)-HETE also induced tyrosine phosphorylation of Janus kinase 2 (Jak2) in VSMCs, and its inhibition substantially reduced STAT3 phosphorylation, MCP-1 expression, and VSMC migration. In addition, Src formed a complex with EGFR and Jak2, and its inhibition completely blocked Jak2 and STAT3 phosphorylation, MCP-1 expression, and VSMC migration. 15(*S*)-HETE induced the production of $H_2O_2$ via an NADPH oxidase-dependent manner and its scavengers, *N*-acetyl cysteine (NAC) and catalase suppressed 15(*S*)-HETE-stimulated EGFR, Src, Jak2, and STAT3 phosphorylation and MCP-1 expression. Balloon injury (BI) induced EGFR, Src, Jak2, and STAT3 phosphorylation, and inhibition of these signaling molecules attenuated BI-induced MCP-1 expression and smooth muscle cell migration from the medial to the luminal surface resulting in reduced neointima formation. In addition, inhibition of EGFR blocked BI-induced Src, Jak2, and STAT3 phosphorylation. Similarly, interference with Src activation suppressed BI-induced Jak2 and STAT3 phosphorylation. Furthermore, adenovirus-mediated expression of dnJak2 also blocked BI-induced STAT3 phosphorylation. Consistent with the effects of 15(*S*)-HETE on the activation of EGFR-Src-Jak2-STAT3 signaling in VSMCs *in vitro*, adenovirus-mediated expression of 15-lipoxygenase 1 (15-Lox1) enhanced BI-induced EGFR, Src, Jak2, and STAT3 phosphorylation leading to enhanced MCP-1 expression *in vivo*. Blockade of Src or Jak2 suppressed BI-induced 15-Lox1-enhanced STAT3 phosphorylation, MCP-1 expression, and neointima formation. In addition, whereas dominant negative Src blocked BI-induced 15-Lox1-enhanced Jak2 phosphorylation, dnJak2 had no effect on Src phosphorylation. Together, these observations demonstrate for the first time that the 15-Lox1–15(*S*)-HETE axis activates EGFR via redox-sensitive manner, which in turn mediates Src-Jak2-STAT3-dependent MCP-1 expression leading to vascular wall remodeling.**

Vascular smooth muscle cell (VSMC)[2] migration and proliferation contribute to the pathogenesis of atherosclerosis and restenosis (1–3). It has been shown that 15-lipoxygenase 1 (15-Lox1) and its murine ortholog 12/15-Lox mediate the oxidation of low density lipoprotein, an important factor in the disease process of atherosclerosis (4, 5). In addition, using transgenic or knock-out mice models, a number of studies have demonstrated that these lipoxygenases indeed play a role in the pathogenesis of both atherosclerosis and restenosis (6–8). Lipoxygenases are non-heme iron dioxygenases that stereospecifically introduce molecular oxygen into polyunsaturated fatty acids, resulting in the formation of hydroperoxyeicosatetraenoic acids, which are subsequently converted to hydroxyeicosatetraenoic acids (HETEs) (9). Furthermore, atherosclerotic arteries upon incubation with arachidonic acid (AA) converted it mainly to 15-HETE (10). Despite the importance of eicosanoids, the oxygenated metabolites of AA, in the maintenance of vascular tone (11, 12) and their increased production in atherosclerotic arteries (10), relatively little is known in regard to their role in vascular wall remodeling. In this regard, studies from our laboratory as well as others have shown that VSMCs express 15-Lox1 and when exposed to AA, convert it primarily to 15(*S*)-HETE (13–15). Furthermore, we have reported that 15(*S*)-HETE is a potent chemotactic molecule to VSMCs and induces the expression of cytokines such as interleukin-6 (IL-6)

* This work was supported, in whole or in part, by National Institutes of Health Grant HL064165 (NHLBI; to G. N. R.).

[1] To whom correspondence should be addressed: Dept. of Physiology, The University of Tennessee Health Sciences Center, 894 Union Ave., Memphis, TN 38163. Tel.: 901-448-7321; Fax: 901-448-7126; E-mail: rgadipar@uthsc.edu.

[2] The abbreviations used are: VSMC, vascular smooth muscle cell; SMC, smooth muscle cell; EGFR, EGF receptor; HETE, hydroxyeicosatetraenoic acid; STAT3, signal transducer and activator of transcription 3; Jak2, Janus kinase 2; NAC, *N*-acetyl cysteine; MCP-1, monocyte chemoattractant protein-1; BI, balloon injury; dn, dominant negative; 15-Lox1, 15-lipoxygenase 1; AA, arachidonic acid; CM-$H_2$DCFDA, 5-(and-6)-chloromethyl-2,7-dichlorodihydrofluorescein diacetate acetyl ester; I/M, intimal/medial; pfu, plaque-forming unit; H & E, hematoxylin and eosin; m.o.i., multiplicity of infection; ROS, reactive oxygen species; Ad, adenovirus.

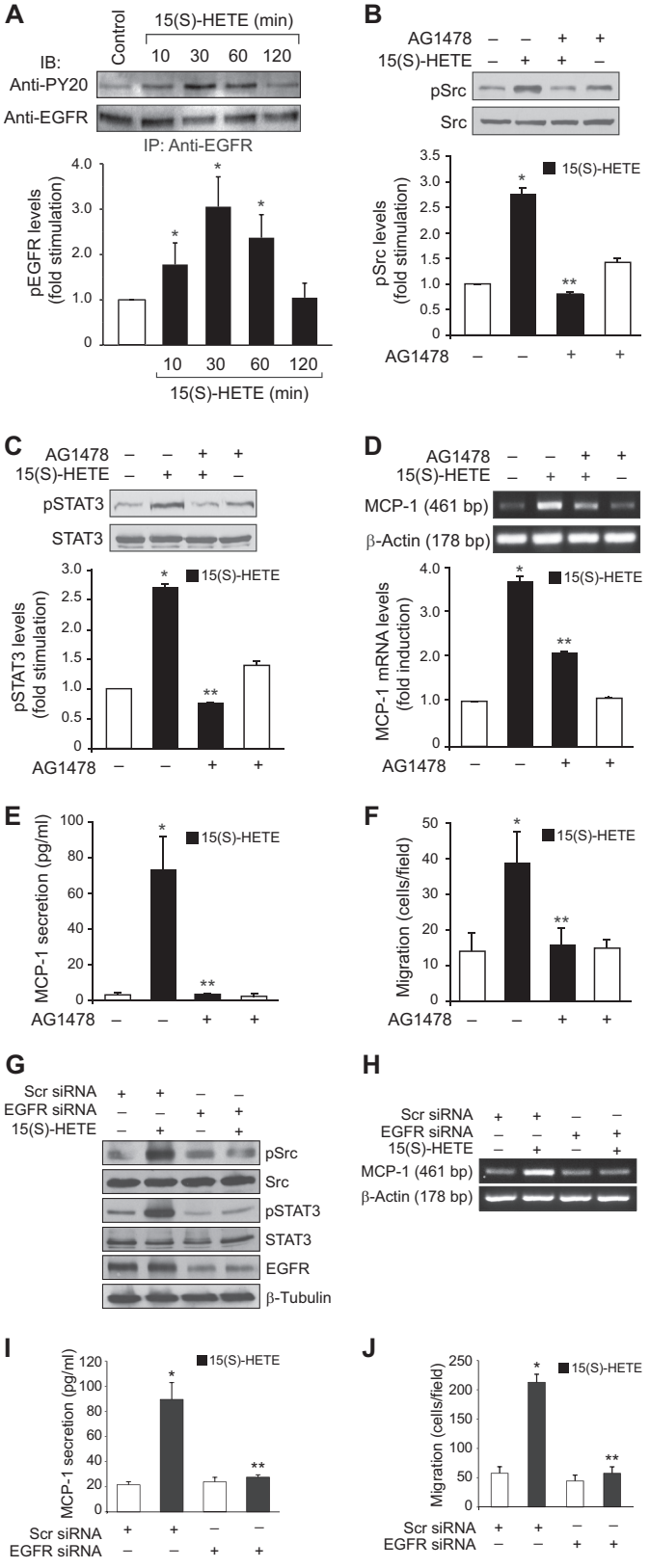


FIGURE 1. **EGFR plays a role in 15(*S*)-HETE-induced Src and STAT3 phosphorylation, MCP-1 expression, and VSMC migration.** *A*, quiescent VSMCs were treated with and without 15(*S*)-HETE (0.5 $\mu$M) for the indicated time periods, cell extracts were prepared, equal amounts of protein from control and each treatment were immunoprecipitated (*IP*) with anti-EGFR antibodies, and the immunocomplexes were analyzed by Western blotting (*IB*) using anti-PY20 antibodies. *B* and *C*, quiescent VSMCs were treated with and without 15(*S*)-HETE (0.5 $\mu$M) in the presence and absence of AG1478 (500 nM) for 30 min, and cell extracts were prepared and analyzed by Western blotting for tyrosine phosphorylation of Src (*B*)and STAT3 (*C*) using their respective phosphotyrosine-specific antibodies. The blots in *panels A–C* were reprobed with anti-EGFR, anti-Src, or anti-STAT3 antibodies for normalization. *D* and *E*, quiescent VSMCs were treated with and without 15(*S*)-HETE (0.5 $\mu$M) in the presence and absence of AG1478 (500 nM) for 2 h, and either total cellular RNA was isolated and analyzed for MCP-1 and $\beta$-actin mRNA levels by RT-PCR (*D*), or media were collected and analyzed for MCP-1 release by ELISA (*E*). *F*, quiescent VSMCs were treated with and without AG1478 (500 nM) for 30 min and subjected to 15(*S*)-HETE (0.5 $\mu$M)-induced migration using a modified Boyden chamber method. *G*, VSMCs that were transfected with scrambled or EGFR siRNA (100 nM) and growth-arrested were treated with and without 15(*S*)-HETE (0.5 $\mu$M) for 30 min, and cell extracts were prepared and analyzed by Western blotting for pSrc and pSTAT3 levels using their respective phosphotyrosine-specific antibodies. The blots were reprobed with anti-Src, anti-STAT3, anti-EGFR, or anti-$\beta$-tubulin antibodies for normalization or to show the effect of EGFR siRNA on its target and non-target molecules. *H* and *I*, all the conditions were the same as in *panel G*, except that cells were treated with and without 15(*S*)-HETE (0.5 $\mu$M) for 2 h and either total cellular RNA was isolated and analyzed for MCP-1 and $\beta$-actin mRNA levels by RT-PCR (*H*) or media were collected and analyzed for MCP-1 release by ELISA (*I*). *J*, all the conditions were the same as in *panel G* except that cells were subjected to 15(*S*)-HETE (0.5 $\mu$M)-induced migration using modified Boyden chamber method. The *bar graphs* represent the mean ± S.D. values of three independent experiments. *, $p < 0.01$ *versus* vehicle or scrambled siRNA control; **, $p < 0.01$ *versus* 15(*S*)-HETE or scrambled siRNA + 15(*S*)-HETE.

and monocyte chemoattractant protein-1 (MCP-1) (16, 17). Our studies have also shown that mitogen-activated protein kinase-mediated cAMP response element binding (CREB) protein and Src-dependent signal transducer and activator of transcription 3 (STAT3) stimulation are required for 15(*S*)-HETE-induced IL-6 and MCP-1 expression, respectively, in VSMCs (16, 17).

Many studies have shown that the Jak family of tyrosine kinases mediates the tyrosine phosphorylation and activation of STATs in the regulation of various cellular responses including cell proliferation and migration in response to a broad range of agonists (18–22). On the other hand, a few studies have reported that the Src family of non-receptor-tyrosine kinases also plays a role in the activation of STATs in response to some agents such as oxidized lipid molecules (23, 24). However, very little is known in regard to the existence of any cross-talk between these two non-receptor-tyrosine kinases in the activation of STAT3. Because our previous studies have indicated that 15(*S*)-HETE activates STAT3 and it requires the involvement of Src, we asked the question of whether Jak2 has any role in these effects, and if so, is there any cross-talk between these two non-receptor-tyrosine kinases in the activation of STAT3? In this report we show that both the tyrosine kinases interact with each other downstream to EGFR in mediating 15-Lox1–15(*S*)-HETE-induced STAT3 activation and MCP-1 expression in VSMCs *in vitro* and in the artery *in vivo*. Our results also demonstrate that EGFR gets activated acutely in the artery after injury alone and with adenovirus-mediated expression of 15-Lox1 and mediates the Src-Jak2-STAT3-MCP-1 signaling axis leading to vascular wall remodeling.

## MATERIALS AND METHODS

*Reagents*—15(*S*)-HETE (34720) was purchased from Cayman Chemicals (Ann Arbor, MI). Allopurinol (A8003), apocynin (4′-hydroxy-3′-methoxyacetophenone) (A10809), catalase-polyethylene glycol (C4963), *N*-acetyl-L-cysteine (NAC)

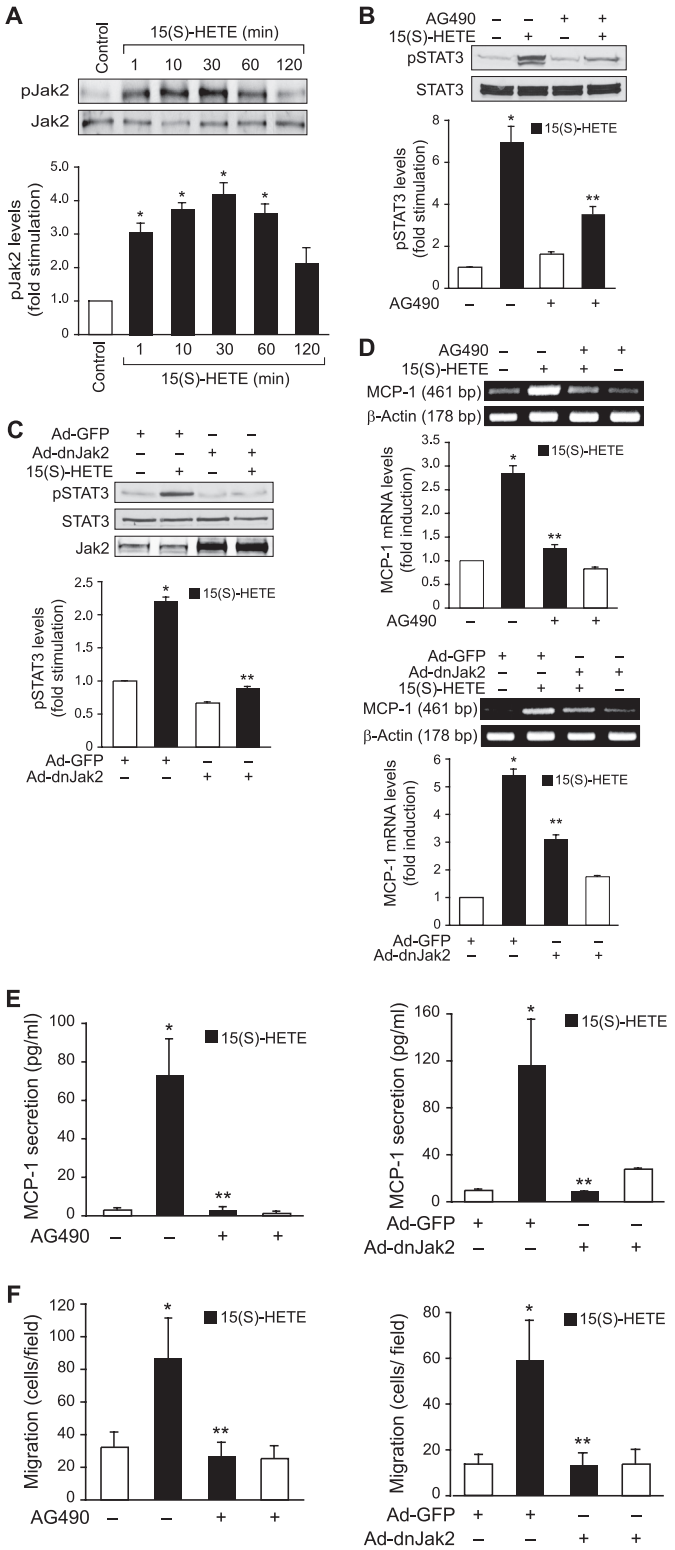


FIGURE 2. **Jak2 plays a role in 15(*S*)-HETE-induced STAT3 phosphorylation, MCP-1 expression, and VSMC migration.** *A* and *B*, quiescent VSMCs were treated with and without 15(*S*)-HETE (0.5 $\mu$M) for the indicated time periods or in the presence and absence of AG490 (25 $\mu$M) for 30 min, and cell extracts were prepared and analyzed by Western blotting for tyrosine phosphorylation of Jak2 (*A*) and STAT3 (*B*) using their respective phosphotyrosine-specific antibodies. *C*, VSMCs that were transduced with Ad-GFP or Ad-dnJak2 at 40 m.o.i. and growth-arrested were treated with and without 15(*S*)-HETE (0.5 $\mu$M) for 30 min, and cell extracts were prepared and analyzed for STAT3 tyrosine phosphorylation as described in *panel B*. The blots in *panels A–C* were reprobed with anti-Jak2 or anti-STAT3 antibodies for normalization or to show overexpression of dominant negative Jak2. *D* and *E*, quiescent VSMCs were treated with and without 15(*S*)-HETE (0.5 $\mu$M) in the presence and absence of AG490 (25 $\mu$M) for 2 h, and either total cellular RNA was isolated and analyzed for MCP-1 and $\beta$-actin mRNA levels by RT-PCR (*D*, *upper panel*) or medium was collected and MCP-1 release was measured by ELISA (*E*, *left panel*). Wherever a dominant negative mutant approach was used to block Jak2 activation, cells were transduced with Ad-GFP or Ad-dnJak2 at 40 m.o.i., growth-arrested, and treated with and without 15(*S*)-HETE (0.5 $\mu$M) for 2 h, and either total cellular RNA was isolated and analyzed for MCP-1 and $\beta$-actin mRNA levels by RT-PCR (*D*, *lower panel*) or medium was collected and MCP-1 release was measured by ELISA (*E*, *right panel*). *F*, quiescent VSMCs that were pretreated with and without AG490 (25 $\mu$M) for 30 min were subjected to 15(*S*)-HETE (0.5 $\mu$M)-induced migration using modified Boyden chamber method (*left panel*). When the effect of Ad-dnJak2 was tested, cells were transduced with Ad-GFP or Ad-dnJak2 at 40 m.o.i., growth-arrested, and subjected to 15(*S*)-HETE (0.5 $\mu$M)-induced migration (*right panel*). The *bar graphs* represent mean ± S.D. values of three independent experiments. *, $p < 0.01$ *versus* vehicle control or Ad-GFP; **, $p < 0.01$ *versus* 15(*S*)-HETE or Ad-GFP + 15(*S*)-HETE.

(A7250), and pluronic F127 (P2443) were purchased from Sigma. Diphenyleneiodonium chloride (BML-CN240) was bought from ENZO Life Sciences (Plymouth Meeting, PA). Anti-phospho-STAT3 (9131), anti-phospho-Src (2101), and anti-Src (2109) antibodies were obtained from Cell Signaling Technology (Beverly, MA). Anti-histone H1 (MAB1276), anti-phospho-Jak2 (09–275), anti-Jak2 (06–255), and anti-phosphotyrosine (05–777) antibodies were obtained from Millipore (Temecula, CA). Anti-STAT3 (SC-482) and anti-EGFR (SC-03) antibodies were purchased from Santa Cruz Biotechnology (Santa Cruz, CA). AG 1478 (658552), AG 490 (658401), PP1 (529579), and Eosin Y (200-12) were bought from EMD Biosciences (Gibbstown, NJ). The rat MCP-1 ELISA kit (KRC1011) and 5-(and-6)-chloromethyl-2,7-dichlorodihydrofluorescein diacetate acetyl ester (CM-$H_2$DCFDA) (C6827) were obtained from Invitrogen. Rat EGFR siRNA (ON-TARGET plus SMARTpool L-080049-01) and scrambled siRNA (ON-TARGET plus Non-targeting Pool) were obtained from Dharmacon RNAi Technologies (Chicago, IL). Hematoxylin (H-3404), biotinylated anti-mouse IgG (BA-9200), ABC kit (PK-6100), and DAB kit (SK-4100) were bought from Vector Laboratories (Burlingame, CA). All primers and oligonucleotides used in this study were synthesized by IDT (Coralville, IA).

*Cell Culture*—Rat VSMCs were isolated and subcultured as described previously (25). VSMCs were used between 6 and 12 passages.

*Adenoviral Vectors*—The construction of Ad-GFP, Ad-dnJak2, Ad-15-Lox1, and Ad-dnSrc were described previously (17, 25–27). The plasmids, pAd-GFP, pAd-dnJak2, pAd-15-Lox1, and pAd-dnSrc were linearized by digestion with PacI and transfected into HEK293A cells. The resultant adenovirus was further amplified by infection of HEK293A cells and purified by cesium chloride gradient ultracentrifugation (28).

*Cell Migration*—Cell migration was measured using a modified Boyden chamber method as described previously (29). Wherever adenovirus was used, cells were infected with the respective adenovirus at an m.o.i. of 40 and growth-arrested before they were subjected to stimulus-induced migration. Cell motility is presented as number of migrated cells per field.

*RT-PCR*—After appropriate treatments, total cellular RNA was isolated from VSMCs using TRIzol reagent as per the man-

ufacturer's instructions (Invitrogen). Reverse transcription was carried out with a High Capacity cDNA Reverse Transcription kit (Applied Biosystems, Foster City, CA). The cDNA was then used as a template for PCR using specific primers. The primers used are as follows: rat MCP-1 (accession number AF058786) forward (5′-CAGAAACCAGCCAACTCTCA-3′) and reverse (5′-GCTTGAGGTGGTTGTGGAAA-3′); rat β-actin (accession number EF156276) forward (5′-CGTTGACATCCGTAAAGACC-3′) and reverse (5′-GATAGAGCCACCAATCCACA-3′). The amplification was carried out on Gene Amp PCR System 2400 (Applied Biosystems). The amplified RT-PCR products were separated on 1.5% (w/v) agarose gels and stained with ethidium bromide, pictures were captured using AlphaEase Digital Imaging System (Alpha Innotech Corporation, San Leandro, CA), and the band intensities were quantified using NIH ImageJ.

*ELISA*—MCP-1 release into medium was measured by using rat MCP-1 ELISA kit following the manufacturer's instructions, and the data are expressed as pg/ml.

*Western Blot Analysis*—After appropriate treatments and rinsing with cold PBS, VSMCs were lysed in 500 μl of lysis buffer (1× PBS, 1% Nonidet P-40, 0.5% sodium deoxycholate, 0.1% SDS, 100 μg/ml aprotinin, 1 μg/ml leupeptin, and 1 mM sodium orthovanadate), and the lysates were collected into 1.5-ml microcentrifuge tubes. After 20 min of incubation on ice, the cell lysates were cleared by centrifugation at 12,000 rpm for 20 min at 4 °C. The cell lysates containing an equal amount of protein were resolved by electrophoresis on 0.1% SDS and 10% polyacrylamide gels. The proteins were electroblotted to a nitrocellulose membrane (Hybond, GE Healthcare). After blocking in 10 mM Tris-HCl buffer, pH 8.0, containing 150 mM sodium chloride, 0.1% Tween 20, and 5% (w/v) nonfat dry milk, the membrane was treated with appropriate primary antibodies followed by incubation with horseradish peroxidase-conjugated secondary antibodies. The antigen-antibody complexes were detected using a chemiluminescence reagent kit (GE Healthcare). The band intensities were quantified using NIH ImageJ.

*ROS Production*—ROS production was measured by using CM-$H_2$DCFDA fluorescence staining (30).

*Carotid Artery Balloon Injury (BI)*—All animal protocols were performed in accordance with the relevant guidelines and regulations approved by the Institutional Animal Care and Use Committee of the University of Tennessee Health Science Center, Memphis, TN. BI was performed essentially as described previously (31). At 3 days or 2 weeks after BI, the animals were sacrificed with an overdose of pentobarbital (200 mg/kg), and the carotid arteries were collected and processed for protein extraction, RNA isolation and/or morphometric analysis. For morphometric analysis, carotid arteries were fixed in 10% formalin and embedded in OCT solution (Sakura Finetek USA Inc., Torrance, CA), and 5-μm-thick sections were made at equally spaced intervals in the middle of injured and uninjured common carotid artery segments and stained with hematoxylin and eosin. The intimal (*I*) and medial (*M*) areas were measured using NIH ImageJ, and the I/M ratios were calculated.

*In Vivo SMC Migration Assay*—The *in vivo* SMC migration was determined as described by Bendeck *et al.* (32). Briefly, 3

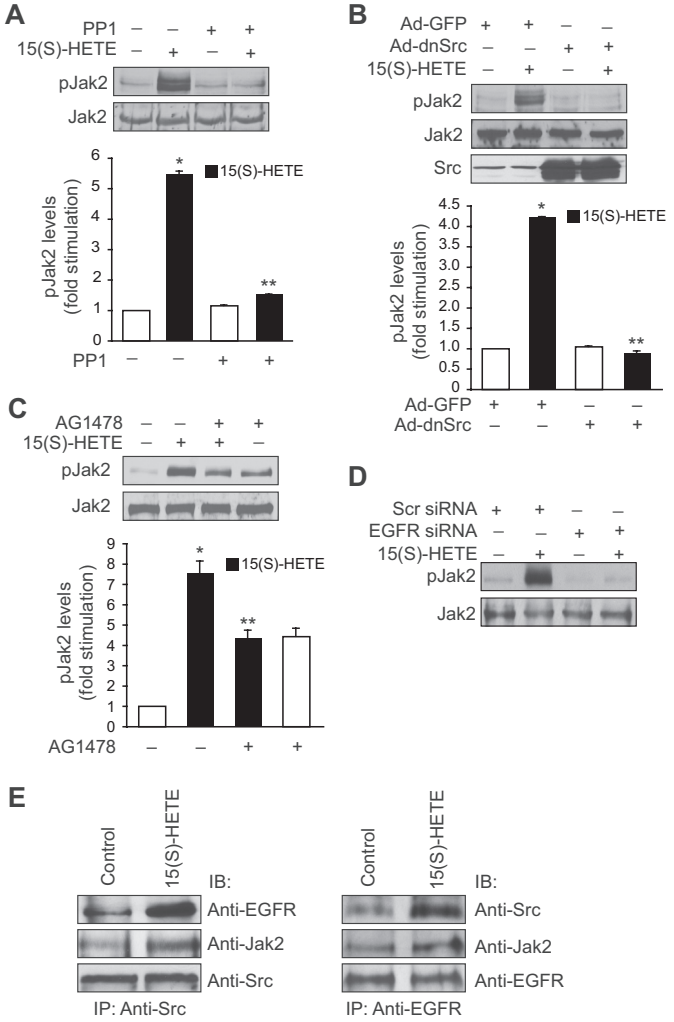


FIGURE 3. **EGFR and Src mediate 15(*S*)-HETE-induced Jak2 phosphorylation.** *A*, quiescent VSMCs were treated with and without 15(*S*)-HETE (0.5 μM) in the presence and absence of PP1 (10 μM) for 30 min, and cell extracts were prepared and analyzed by Western blotting for Jak2 tyrosine phosphorylation using its phosphotyrosine-specific antibodies. *B*, all the conditions were the same as in *panel A* except that cells were transduced with Ad-GFP or Ad-dnSrc at 40 m.o.i. and growth-arrested before subjecting them to treatment with or without 15(*S*)-HETE and analyzing for Jak2 tyrosine phosphorylation. *C*, quiescent VSMCs were treated with and without 15(*S*)-HETE (0.5 μM) in the presence and absence of AG1478 (500 nM) for 30 min, and cell extracts were prepared and analyzed for tyrosine phosphorylation of Jak2 as described in *panel A*. *D*, VSMCs that were transfected with scrambled or EGFR siRNA (100 nM) and growth-arrested were treated with and without 15(*S*)-HETE (0.5 μM) for 30 min, and cell extracts were prepared and analyzed by Western blotting for Jak2 tyrosine phosphorylation as described in *panel A*. *E*, quiescent VSMCs were treated with and without 15(*S*)-HETE (0.5 μM) for 30 min, and cell extracts were prepared. An equal amount of protein from control and each treatment was then subjected to immunoprecipitation (*IP*) with anti-Src or anti-EGFR antibodies, and the resulting immunocomplexes were analyzed by Western blotting (*IB*) for EGFR, Jak2, and Src using their specific antibodies. The blots in *panels A–D* were reprobed with anti-Jak2 or anti-Src antibodies for normalization or to show overexpression of dominant negative Src. *Bar graphs* represent the mean ± S.D. values of three independent experiments. *, $p < 0.01$ *versus* vehicle control or Ad-GFP; **, $p < 0.01$ *versus* 15(*S*)-HETE or Ad-GFP + 15(*S*)-HETE.

days after BI, the carotid arteries were fixed *in vivo* with 10% buffered formalin at physiological pressure. The middle 1 cm of the denuded (injured) common carotid artery was cut and fixed in cold acetone for 10 min. The artery was then opened longitudinally and pinned down onto an agar plate with the luminal surface facing upward. The arteries were rinsed in PBS and then

placed in 0.3% $H_2O_2$ for 30 min to block endogenous peroxidase activity. Nonspecific protein binding was blocked by incubating the arteries in 5% normal goat serum in PBS for 30 min. The arteries were incubated with anti-histone H1 antibodies diluted 1:300 in PBS for 1 h followed by incubation with biotinylated goat anti-mouse IgG for 30 min. Peroxidase labeling was carried

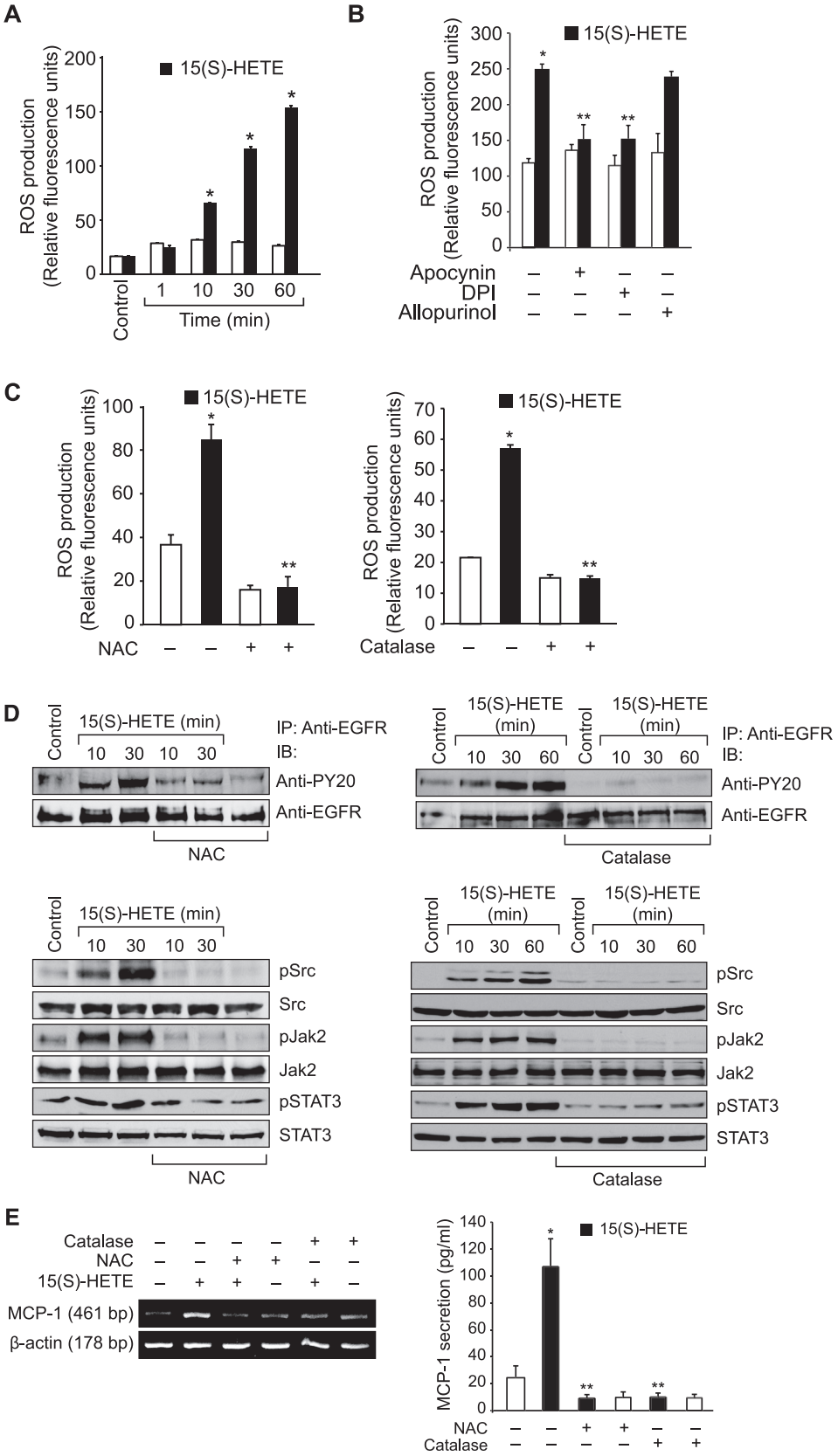

out by using ABC kit (Vector Laboratories), and the signals were visualized by using DAB kit (Vector Laboratories). After each step, the slides were rinsed 3 times for 5 min each in PBS. Finally, the opened arteries were placed intimal side up on glass slides with coverslips. As a negative control, samples of the same specimens without the primary antibody incubation were used. The intimal surface of the vessel was examined under a light microscope at X200 magnification, and the total number of positively stained cells per 0.1 $mm^2$ of the luminal surface area was counted.

*Delivery of Adenovirus into Injured Arteries*—After BI, solutions of 100 $\mu$l of Ad-GFP ($10^{10}$ pfu/ml) Ad-dnJak2 ($10^{10}$ pfu/ml), or Ad-dnSrc ($10^{10}$ pfu/ml) were infused into the ligated segment of the common carotid artery for 30 min as described previously (25).

*Statistics*—All the experiments were repeated three times with similar results. Data are presented as the means ± S.D. The treatment effects were analyzed by Student's *t* test. *p* values $<0.05$ were considered to be statistically significant. In the case of Western blotting, histochemistry, and RT-PCR, one of the representative sets of data is shown.

## RESULTS

*15(S)-Hydroxyeicosatetraenoic Acid Stimulates Tyrosine Phosphorylation of EGFR*—To understand the mechanisms by which the 15-Lox1 metabolite of AA, 15(*S*)-HETE, induces Src-STAT3 signaling leading to VSMC migration, we have studied the role of EGFR. 15(*S*)-HETE stimulated tyrosine phosphorylation of EGFR in a time-dependent manner (Fig. 1*A*). AG1478, a potent inhibitor of EGFR (33), blocked 15(*S*)-HETE-induced Src (Tyr-416) and STAT3 (Tyr-705) phosphorylation (Fig. 1, *B* and *C*). Similarly, AG1478 inhibited 15(*S*)-HETE-induced MCP-1 expression both at mRNA and protein levels (Fig. 1, *D* and *E*). Consistent with its effects on Src and STAT3 phosphorylation and MCP-1 expression, AG1478 also inhibited VSMC migration (Fig. 1*F*). To substantiate the role of EGFR in (15(*S*)-HETE-induced Src and STAT3 phosphorylation and MCP-1 expression, we used the siRNA approach. Down-regulation of EGFR by its siRNA led to inhibition of 15(*S*)-HETE-induced Src and STAT3 phosphorylation and MCP-1 expression (Fig. 1, *G–I*). Depletion of EGFR levels also attenuated 15(*S*)-HETE-induced VSMC migration (Fig. 1*J*).

*15(S)-Hydroxyeicosatetraenoic Acid Stimulates Tyrosine Phosphorylation of Jak2*—A large body of data indicates that the Jak family of tyrosine kinases plays a major role in agonist-induced STAT3 phosphorylation (18–22). Therefore, to find the involvement of the Jak family of tyrosine kinases in 15(*S*)-HETE-induced STAT3 activation, we studied the role of Jak2. 15(*S*)-HETE induced tyrosine phosphorylation of Jak2 (Tyr1007/1008) in a time-dependent manner (Fig. 2*A*). Next we used both pharmacological and dominant negative mutant approaches to test the role of Jak2 in STAT3 phosphorylation. AG490, a potent inhibitor of Jak2 (34), suppressed 15(*S*)-HETE-induced STAT3 phosphorylation (Fig. 2*B*). Similarly, adenovirus-mediated expression of dominant negative Jak2 inhibited 15(*S*)-HETE-induced STAT3 phosphorylation (Fig. 2*C*). Blockade of Jak2 activation by either approach also inhibited 15(*S*)-HETE-induced MCP-1 expression and its release by VSMCs, which in turn affected the migration of these cells (Fig. 2, *D–F*).

*15(S)-Hydroxyeicosatetraenoic Acid-induced STAT3 Phosphorylation Requires Activation of Both Src and Jak2*—Because inhibition of either Src or Jak2 attenuated STAT3 phosphorylation, we were intrigued to find whether there is any cross-talk between these two non-receptor-tyrosine kinases. To test this possibility, we studied the role of Src in 15(*S*)-HETE-induced Jak2 phosphorylation. PP1, a potent inhibitor of Src (24), abolished Jak2 phosphorylation by 15(*S*)-HETE (Fig. 3*A*). Consistent with this observation, adenovirus-mediated expression of dnSrc also suppressed 15(*S*)-HETE-induced Jak2 phosphorylation (Fig. 3*B*). To find a connection between Jak2 and EGFR, we tested the effect of AG1478 on 15(*S*)-HETE-induced Jak2 phosphorylation. AG1478 completely inhibited 15(*S*)-HETE-induced Jak2 phosphorylation (Fig. 3*C*). Furthermore, down-regulation of EGFR levels by its siRNA also attenuated 15(*S*)-HETE-induced Jak2 phosphorylation (Fig. 3*D*). To test whether EGFR, Src, and Jak2 form a complex in response to 15(*S*)-HETE, we performed co-immunoprecipitation assays. Immunoblotting of anti-Src immunoprecipitates of control and 15(*S*)-HETE-treated VSMCs for EGFR showed a band with a molecular mass of 170 kDa whose intensity was found to be higher in 15(*S*)-HETE-treated cells compared with control (Fig. 3*E*). Sequential probing of this membrane with anti-Jak2 antibodies revealed the association of both EGFR and Jak2 with Src. The association of Src and Jak2 with EGFR was further confirmed by immunoblotting of anti-EGFR immunoprecipitates of control and 15(*S*)-HETE-treated VSMCs with anti-Src and anti-Jak2 antibodies (Fig. 3*E*).

*15(S)-Hydroxyeicosatetraenoic Acid-induced EGFR-Src-Jak2-STAT3 Phosphorylation and MCP-1 Expression Require Reactive Oxygen Species (ROS) Production*—To understand the mechanism(s) of activation of EGFR-Src-Jak2-STAT3 signaling by 15(*S*)-HETE, we tested its effect on ROS production. 15(*S*)-HETE induced the production of ROS in a time-dependent manner (Fig. 4*A*). To find the cellular source of 15(*S*)-HETE-induced ROS production, we tested the role of NADPH oxi-

FIGURE 4. **15(*S*)-HETE-induced EGFR-Src-Jak2-STAT3 tyrosine phosphorylation and MCP-1 expression require ROS production.** *A* and *B*, quiescent VSMCs were treated with and without 15(*S*)-HETE (0.5 $\mu$M) for the indicated time periods (*A*) or in the presence and absence of apocynin (100 $\mu$M), DPI (10 $\mu$M), or allopurinol (100 $\mu$M) for 30 min (*B*), and ROS production was measured by CM-$H_2$DCFDA fluorescence staining. *C*, all the conditions were the same as in *panels A* and *B*, except that cells were pretreated with NAC (10 mM) or peg-catalase (6000 units/ml) for 6 h at which time the cells were treated with or without 15(*S*)-HETE (0.5 $\mu$M) for 30 min and the ROS production was measured. *D*, quiescent VSMCs that were preincubated with and without NAC (10 mM) or peg-catalase (6000 units/ml) for 6 h were treated with and without 15(*S*)-HETE (0.5 $\mu$M) for the indicated times, and cell extracts were prepared. Cell extracts containing an equal amount of protein from each were either immunoprecipitated (*IP*) with anti-EGFR antibodies followed by immunoblotting (*IB*) with anti-PY-20 antibodies or subjected to Western blot analysis for pSrc, pJak2, and pSTAT3 using their phosphotyrosine-specific antibodies. The blots were reprobed with anti-EGFR, anti-Src, anti-Jak2, or anti-STAT3 antibodies for normalization. *E*, all the conditions were the same as in *panel D*, except that cells were treated with or without 15(*S*)-HETE (0.5 $\mu$M) for 2 h, and either RNA was isolated and analyzed for MCP-1 and $\beta$-actin mRNA levels by RT-PCR or medium was collected and analyzed for MCP-1 secretion by ELISA. *, $p < 0.01$ *versus* control; **, $p < 0.01$ *versus* 15(*S*)-HETE.

dase. Apocynin and diphenyleneiodonium chloride (DPI), two structurally dissimilar inhibitors of NADPH oxidase (30, 35), but not allopurinol, a specific inhibitor of xanthine oxidase (36), completely blocked 15(*S*)-HETE-induced ROS production (Fig. 4*B*). This result infers that 15(*S*)-HETE induces ROS production via activation of NADPH oxidase. To identify the ROS species, we next used NAC and catalase, a nonspecific and specific scavengers of $H_2O_2$ (37). Both scavengers neutralized the production of ROS by 15(*S*)-HETE, suggesting that the ROS species produced by this lipid molecule is $H_2O_2$ (Fig. 4*C*). NAC and catalase also blocked 15(*S*)-HETE-induced EGFR, Src, Jak2, and STAT3 tyrosine phosphorylation and MCP-1 expression (Fig. 4, *D* and *E*).

*Inhibition of EGFR Activation Abrogates BI-induced Src, Jak2, and STAT3 Phosphorylation and MCP-1 Expression*—To understand the role of EGFR in Src-Jak2-STAT3 signaling *in vivo*, we used rat carotid BI model. BI induced tyrosine phosphorylation of EGFR, Src, Jak2, and STAT3 (Fig. 5*A*). Administration of AG1478 soon after BI inhibited Src, Jak2, and STAT3 phosphorylation almost completely (Fig. 5*A*). BI also induced MCP-1 expression, and this response was blocked by AG1478 (Fig. 5*B*). Consistent with these observations, blockade of EGFR reduced migration of SMC from medial to intimal region and neointima formation (Fig. 5, *C* and *D*). Similarly, adenovirus-mediated transduction of either dnSrc or dnJak2 inhibited BI-induced STAT3 phosphorylation, MCP-1 expression, and SMC migration from medial to intimal region resulting in the suppression of neointima formation (Figs. 6, *A–D*, and 7, *A–D*). Furthermore, inhibition of Src blocked BI-induced Jak2 phosphorylation (Fig. 6*A*). To relate these signaling events to 15(*S*)-HETE in the artery, we also tested the effect of 15-Lox1 overexpression on EGFR, Src, Jak2, and STAT3 tyrosine phosphorylation and MCP-1 expression. Adenovirus-mediated transduction of 15-Lox1 enhanced BI-induced EGFR, Src, Jak2, and STAT3 tyrosine phosphorylation and MCP-1 expression (Fig. 8, *A–C*). Treatment of contra-lateral artery with Ad-15-Lox1 alone without BI did not cause any neointima formation (data not shown). In addition, adenovirus-mediated expression of dn-Src or dn-Jak2 suppressed 15-Lox1-enhanced STAT3 tyrosine phosphorylation, MCP-1 expression, and neointima formation (Fig. 8, *D–F*). Although dnSrc blocked 15-Lox1-enhanced Jak2 tyrosine phosphorylation, dn-Jak2 had no effect on Src tyrosine phosphorylation (Fig. 8*D*).

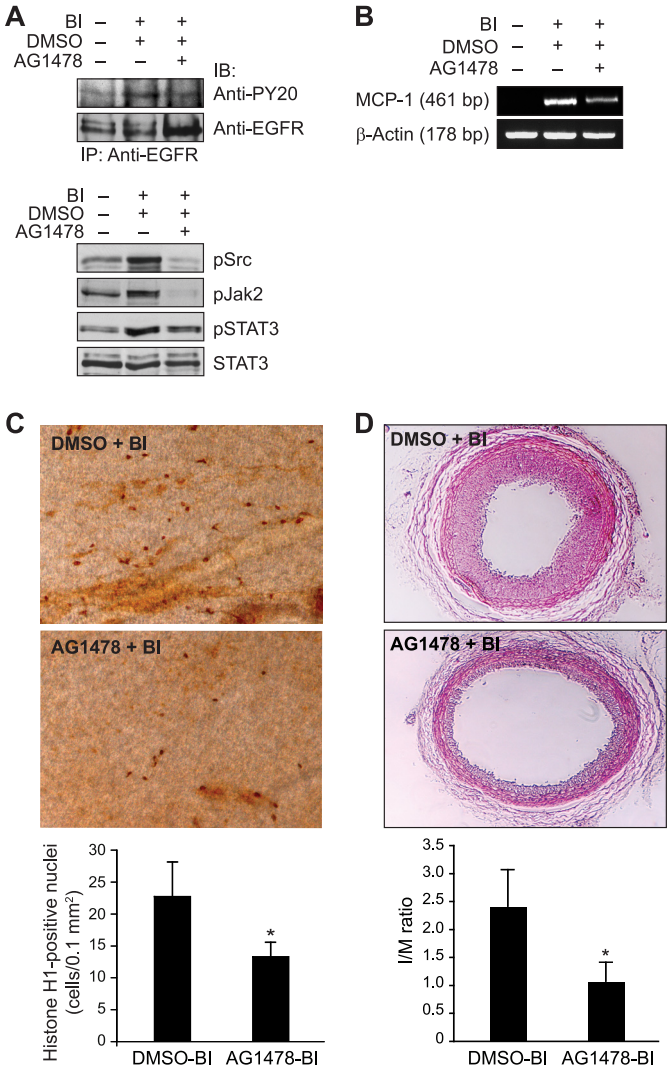


FIGURE 5. **Inhibition of EGFR suppresses BI-induced Src, Jak2, and STAT3 phosphorylation and MCP-1 expression leading to decreased migration of SMC from medial to luminal region and neointima formation.** *A*, 24 h after BI and administration of vehicle or AG1478 (5 $\mu$M), the rats were sacrificed, and the injured and uninjured common carotid arteries were dissected out and tissue extracts were prepared. AG1478 was delivered via mixing with 30% (w/v) pluronic gel and applied around the injured artery. *Upper panel*, tissue extracts containing equal amounts of proteins were immunoprecipitated (*IP*) with anti-EGFR antibodies, and the immunocomplexes were analyzed by Western blotting (*IB*) with anti-PY20 antibodies. *Lower panel*, an equal amount of protein from each condition was analyzed for tyrosine phosphorylation of Src, Jak2, and STAT3 by Western blotting using their phosphotyrosine-specific antibodies. The blots in both panels were reprobed with anti-EGFR or anti-STAT3 antibodies for normalization. *B*, all the conditions were the same as in *panel A*, except that RNA was isolated and analyzed for MCP-1 and $\beta$-actin expression by RT-PCR. *C*, 3 days after BI and administration with vehicle or AG1478 (5 $\mu$M), injured common carotid arteries were isolated, opened longitudinally, and stained with anti-histone H1 antibodies, and histone H1-positive nuclei were counted. *D*, 2 weeks after BI and administration with vehicle or AG1478 (5 $\mu$M), rats were sacrificed, arteries were isolated, fixed, cross-sections made and stained with H & E. After morphometry analysis, the I/M ratios were calculated. The *upper panel* shows the representative pictures of balloon-injured carotid artery cross-sections that were stained with H & E. The *bar graph* in the *bottom panel* shows the quantitative analysis of the I/M ratios of the carotid arteries. *, $p < 0.05$ *versus* DMSO-BI ($n = 6$).

## DISCUSSION

The important findings of the present study are as follows. 1) 15(*S*)-HETE induced tyrosine phosphorylation of EGFR in a time-dependent manner. 2) Blockade of EGFR activation inhibited 15(*S*)-HETE-induced Src and STAT3 tyrosine phosphorylation, MCP-1 expression, and VSMC migration. 3) 15(*S*)-HETE also induced tyrosine phosphorylation of Jak2 and interference with its activation resulted in down-regulation of STAT3 activation, MCP-1 expression, and VSMC migration. 4) Inhibition of Src suppressed 15(*S*)-HETE-induced Jak2 tyrosine phosphorylation. 5) 15(*S*)-HETE induced the production of $H_2O_2$ in a time- and NADPH oxidase-dependent manner in VSMCs. 6) $H_2O_2$ scavengers, NAC and catalase, blocked 15(*S*)-HETE-induced EGFR, Src, Jak2, and STAT3 tyrosine phosphorylation and MCP-1 expression. 7) BI induced EGFR, Src, Jak2, and STAT3 tyrosine phosphorylation and MCP-1 expression. 8) Administration of EGFR inhibitor AG1478 attenuated BI-induced Src, Jak2, and STAT3 tyrosine phosphorylation and

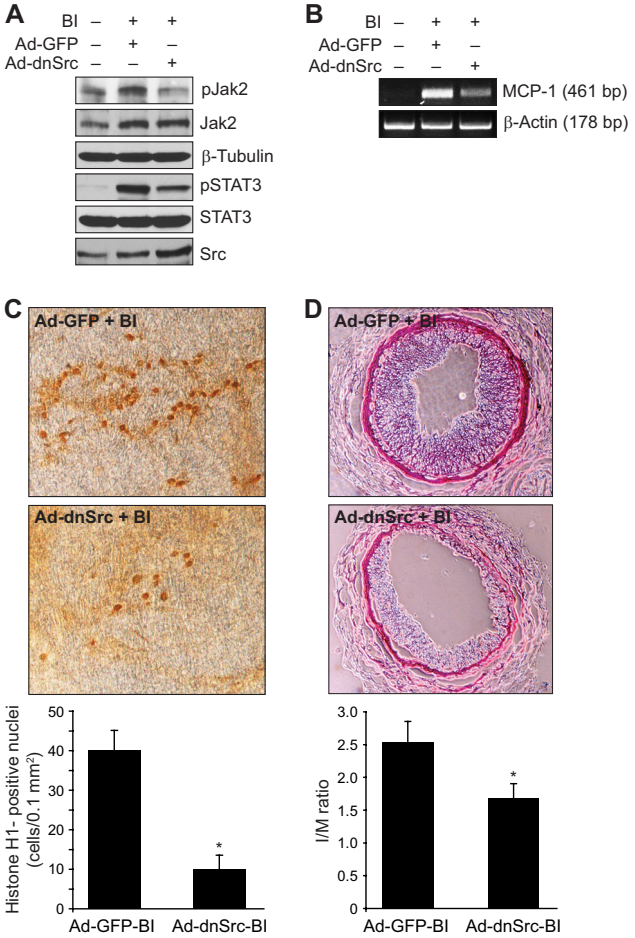


FIGURE 6. **Blockade of Src in rat carotid arteries inhibits BI-induced Jak2 and STAT3 phosphorylation as well as MCP-1 expression leading to decreased migration of SMC from medial to luminal region and neointima formation.** *A* and *B*, 3 days after BI and transduction with Ad-GFP ($10^{10}$ pfu) or Ad-dnSrc ($10^{10}$ pfu), the uninjured and injured common carotid arteries were isolated, and either tissue extracts were prepared and analyzed for Jak2 and STAT3 phosphorylation using their phosphotyrosine-specific antibodies (*A*) or RNA was isolated and analyzed for MCP-1 and β-actin expression by RT-PCR (*B*). The blots in *panel A* were reprobed with anti-Jak2, anti-β-tubulin, anti-STAT3, or anti-Src antibodies for normalization or to show overexpression of dnSrc. *C*, all the conditions were the same as in *panel A*, except that after isolation, arteries were opened longitudinally and stained with anti-histone H1 antibodies, and histone H1-positive nuclei were counted. *D*, 2 weeks after BI and transduction with Ad-GFP ($10^{10}$ pfu) or Ad-dnSrc ($10^{10}$ pfu), rats were sacrificed, arteries were isolated, fixed, cross-sections made and stained with H & E. After morphometry analysis, the I/M ratios were calculated. The *upper panel* shows the representative pictures of balloon-injured Ad-GFP- or Ad-dnSrc-transduced carotid artery cross-sections that were stained with H & E. The *bar graph* in the *bottom panel* shows the quantitative analysis of the I/M ratios of the carotid arteries. *, $p < 0.05$ *versus* Ad-GFP-BI ($n = 6$).

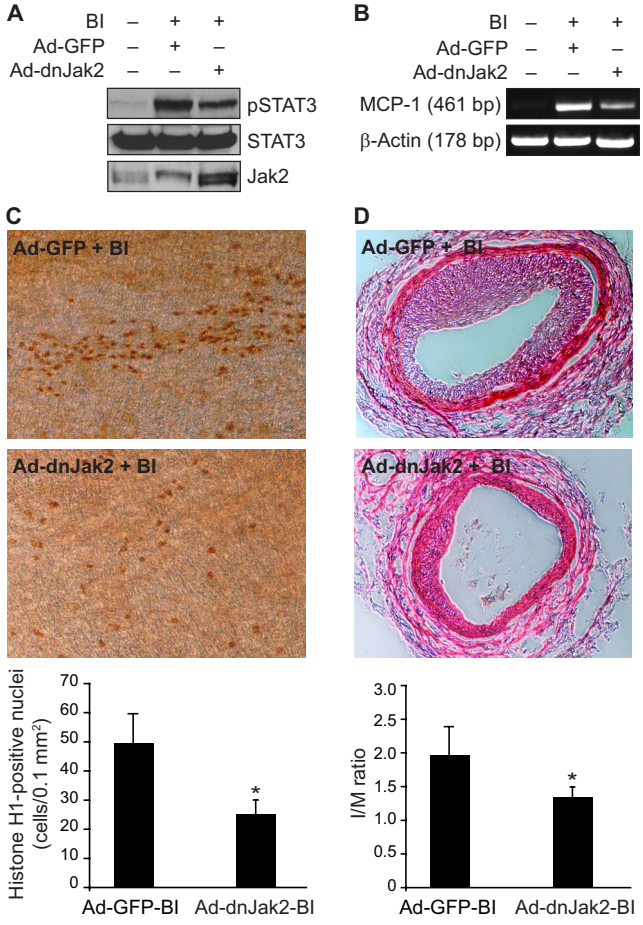


FIGURE 7. **Blockade of Jak2 in rat carotid arteries inhibits BI-induced STAT3 phosphorylation and MCP-1 expression leading to decreased migration of SMC from medial to luminal region and neointima formation.** *A* and *B*, 3 days after BI and transduction with Ad-GFP ($10^{10}$ pfu) or Ad-dnJak2 ($10^{10}$ pfu), the uninjured and injured common carotid arteries were isolated, and either tissue extracts were prepared and analyzed for STAT3 phosphorylation using its phosphotyrosine-specific antibodies (*A*) or RNA was isolated and analyzed for MCP-1 and β-actin expression by RT-PCR (*B*). The *blot* in *panel A* was sequentially reprobed with anti-STAT3 and anti-Jak2 antibodies for normalization or to show overexpression of dnJak2. *C*, all the conditions were the same as in *panel A* except that after isolation, arteries were opened longitudinally and stained with anti-histone H1 antibodies, and histone H1-positive nuclei were counted. *D*, 2 weeks after BI and transduction with Ad-GFP ($10^{10}$ pfu) or Ad-dnJak2 ($10^{10}$ pfu), rats were sacrificed, arteries were isolated, fixed, cross-sections made and stained with H & E. After morphometry analysis, the I/M ratios were calculated. The *upper panel* shows the representative pictures of balloon-injured Ad-GFP- or Ad-dnJak2-transduced carotid artery cross-sections that were stained with H & E. The *bar graph* in the *bottom panel* shows the quantitative analysis of the I/M ratios of the carotid arteries. *, $p < 0.05$ *versus* Ad-GFP-BI ($n = 6$).

MCP-1 expression, resulting in reduced SMC migration from media to intima region and neointima formation. 9) Inhibition of Src via adenovirus-mediated transduction of its dominant negative mutant attenuated BI-induced Jak2 and STAT3 tyrosine phosphorylation, SMC migration from media to intima region, and neointima formation. 10) Interference with activation of Jak2 also reduced STAT3 tyrosine phosphorylation, SMC migration from media to intima region, and neointima formation. 11) Adenovirus-mediated expression of 15-Lox1 enhanced BI-induced EGFR, Src, Jak2, and STAT3 phosphorylation, MCP-1 expression, and neointima formation. 12) Adenovirus-mediated transduction of either dn-Src or dnJak2 suppressed BI-induced 15-Lox1-enhanced STAT3 tyrosine phosphorylation, MCP-1 expression, and neointima formation. The role of EGFR in mediating intracellular signaling events such as the activation of extracellular signal-regulated kinases in response to a variety of agents, including G protein-coupled receptor (GPCR) agonists and oxidants, has been reported (3, 33, 38–40). The capacity of 15(*S*)-HETE in the activation of EGFR and suppression of Src-Jak2-STAT3-MCP-1 signaling by EGFR inhibitor AG1478 or its siRNA suggest that EGFR mediates 15(*S*)-HETE-induced tyrosine phosphorylation-dependent signaling events leading to MCP-1 expression and VSMC

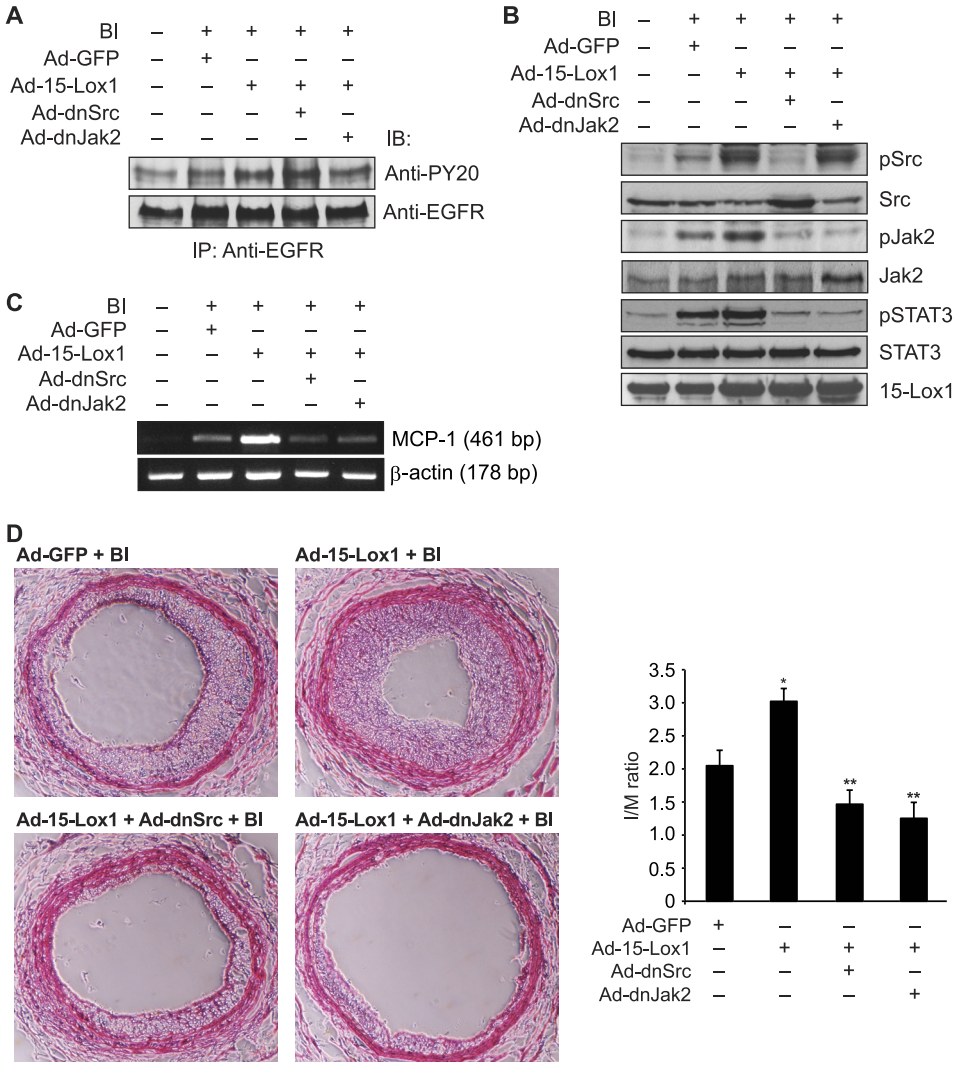


FIGURE 8. **Overexpression of 15-Lox1 enhances BI-induced EGFR, Src, Jak2 and STAT3 tyrosine phosphorylation, MCP-1 expression, and neointima formation.** *A–C*, 3 days after BI and transduction with Ad-GFP ($10^{10}$ pfu) alone or Ad-15-Lox1 ($10^{10}$ pfu) with or without Ad-dnSrc ($10^{10}$ pfu) or Ad-dnJak2 ($10^{10}$ pfu) combination, the uninjured and injured common carotid arteries were isolated, and either tissue extracts were prepared and analyzed for EGFR (*panel A*) and Src, Jak2, and STAT3 (*panel B*) tyrosine phosphorylations as described in Fig. 4, *panel D*, or RNA was isolated and analyzed for MCP-1 and β-actin mRNA levels (*panel C*) as described in Fig. 1, *panel D*. *IP*, immunoprecipitation; *IB*, immunoblot. *D*, all the conditions were the same as in *panel A*, except that arteries were isolated 2 weeks after BI and analyzed for neointima as described in Fig. 7, *panel D*. The *bar graph* shows the quantitative analysis of the I/M ratios of the carotid arteries. The blot in *panel A* was reprobed with normal EGFR antibodies, and the blots in *panel B* were reprobed with normal Src, Jak2, STAT3, or 12-Lox antibodies for normalization or to show the overexpression of 15-lox1. *, $p < 0.05$ *versus* Ad-GFP; **, $p < 0.05$ *versus* Ad-15-Lox1 ($n = 6$).

migration. In regard to understanding the mechanisms of activation of EGFR-Src-Jak2-STAT3-MCP-1 signaling by 15(*S*)-HETE, we observed that it induces the production of ROS in NADPH oxidase-dependent manner. Furthermore, the quenching effect of NAC and catalase on 15(*S*)-HETE-induced ROS production suggests that the ROS species produced by 15(*S*)-HETE is $H_2O_2$. Because 15(*S*)-HETE induced the production of $H_2O_2$, and its scavengers NAC and catalase abolished 15(*S*)-HETE-induced EGFR, Src, Jak2, and STAT3 phosphorylation and MCP-1 expression, it is likely that $H_2O_2$ mediates 15(*S*)-HETE-stimulated EGFR-Src-Jak2-STAT3-MCP-1 signaling in VSMCs. This conclusion can be further supported by our previous observations that oxidants such as $H_2O_2$ stimulate tyrosine phosphorylation of EGFR (40). Many lipid molecules such as lysophosphatidic acid and shingosine 1-phosphate that are coupled to GPCRs transactivate EGFR in many cell types (38, 41). Although no putative receptor has been identified for HETEs thus far, based on the capacity of 15(*S*)-HETE to activate EGFR, one cannot rule out a role for a GPCR in the signaling events of this oxidized lipid molecule. Indeed, some reports have shown that it binds to leukotriene B4 low affinity receptor, BLT2, a GPCR (42).

Based on the large body of data, the Jak family of tyrosine kinases was thought to be the major mediator of activation of STATs in response to a variety of stimulants (18, 21). However, a few studies have shown that besides the Jak family of tyrosine kinases, other non-receptor-tyrosine kinases such as the Src family of tyrosine kinases can also mediate tyrosine phosphorylation and activation of STATs (43). In this aspect we have previously shown that 15(*S*)-HETE stimulates STAT3 tyrosine phosphorylation via activation of Src in both VSMCs and endothelial cells (17, 44). However, what is not known in this aspect is whether there is any interaction between these two non-receptor-tyrosine kinases in the stimulant-mediated STAT3

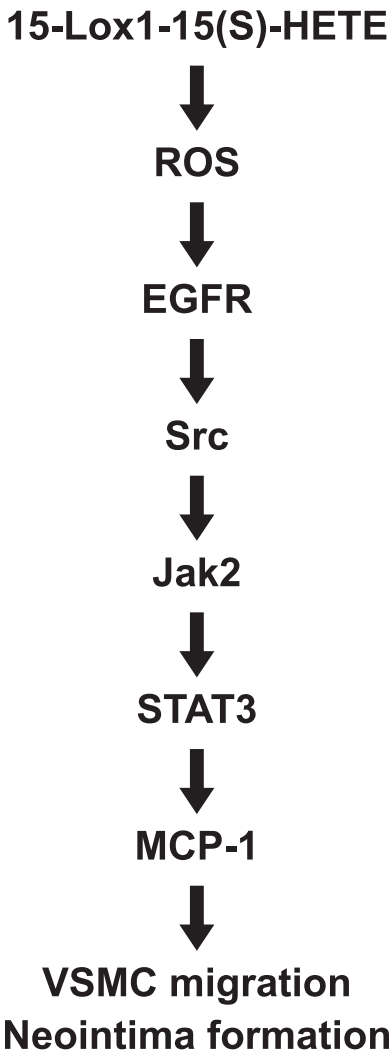


FIGURE 9. **Schematic diagram showing the proposed 15-Lox1–15(*S*)-HETE-ROS-EGFR-Src-Jak2-STAT3-MCP-1 signaling in the mediation of vascular wall remodeling in response to mechanical injury.**

tyrosine phosphorylation and activation? In this regard, our results provide the first direct evidence for the role of Src in the activation of Jak2, at least in response to 15(*S*)-HETE, in VSMCs. In addition, both Src and Jak2 form a complex with each other as well as with EGFR and mediate STAT3 tyrosine phosphorylation. In view of these results, it appears that both Src and Jak2 may lie in the same signaling axis downstream to EGFR in the tyrosine phosphorylation and activation of STATs. The interaction between Src and Jak2 can also be seen at the level of STAT3 target gene, MCP-1, as inhibition of either of these non-receptor-tyrosine kinases suppressed its expression and secretion equally.

Although many studies have reported that GPCR agonists such as angiotensin II, thrombin, and sphingosine 1-phosphate transactivate EGFR in VSMCs (17, 40, 42), the function of EGFR in vascular wall remodeling has not been addressed adequately. In this regard our present results provide compelling evidence for the activation of EGFR in the artery in response to mechanical injury. In addition, activation of EGFR by injury is sufficient in mediating the signaling events such as the Src-Jak2-STAT3 signaling leading to MCP-1 expression, as these events were all sensitive to suppression by its inhibitor AG1478. Furthermore, inhibition of EGFR resulted in the reduction of injury-induced neointima formation. In understanding the role of 15-Lox1–15(*S*)-HETE axis in vascular wall remodeling, previously we have shown that adenovirus-mediated transduction of 15-Lox1 into artery enhances injury-induced neointima formation. In the present study, our results show that adenovirus-mediated transduction of 15-Lox1 into artery also enhances injury-induced EGFR, Src, Jak2, and STAT3 tyrosine phosphorylation as well as MCP-1 expression. Interestingly, EGFR has also been found to be activated in the artery in response to injury in a manner that is dependent on thrombin activity (45). In another study it was reported that blockade of EGFR function by its neutralizing antibodies attenuates injury-induced neointima formation (46). Furthermore, we and others have demonstrated that STAT3 mediates VSMC growth and migration in response to various agents *in vitro* and neointima formation in response to injury *in vivo* (30, 47–50). In addition, the present study demonstrates that 15-Lox1–15(*S*)-HETE axis-mediated vascular wall remodeling requires ROS-dependent activation of EGFR, which in turn targets the stimulation of the Src-Jak2-STAT3 signaling leading to MCP-1 expression. Based on these observations, it is conceivable that various cues target EGFR in relaying their signaling events to the effector molecules in the intact artery in response to injury. Thus, EGFR appears to play a central role in vascular wall remodeling after injury and, therefore, could be a potential target for the development of drugs against vascular lesions such as restenosis.

In summary, as shown in Fig. 9, 15-Lox1–15(*S*)-HETE influences neointima formation via producing ROS and thereby modulating EGFR-Src-Jak2-STAT3-MCP-1 signaling in response to mechanical injury to the artery.

## REFERENCES

1. Newby, A. C., and Zaltsman, A. B. (2000) *J. Pathol.* **190,** 300–309
2. Reape, T. J., and Groot, P. H. (1999) *Atherosclerosis* **147,** 213–225
3. Schwartz, S. M., deBlois, D., and O'Brien, E. R. (1995) *Circ. Res.* **77,** 445–465
4. Ylä-Herttuala, S., Rosenfeld, M. E., Parthasarathy, S., Glass, C. K., Sigal, E., Witztum, J. L., and Steinberg, D. (1990) *Proc. Natl. Acad. Sci. U.S.A.* **87,** 6959–6963
5. Zhu, H., Takahashi, Y., Xu, W., Kawajiri, H., Murakami, T., Yamamoto, M., Iseki, S., Iwasaki, T., Hattori, H., and Yoshimoto, T. (2003) *J. Biol. Chem.* **278,** 13350–13355
6. Cyrus, T., Witztum, J. L., Rader, D. J., Tangirala, R., Fazio, S., Linton, M. F., and Funk, C. D. (1999) *J. Clin. Invest.* **103,** 1597–1604
7. Harats, D., Shaish, A., George, J., Mulkins, M., Kurihara, H., Levkovitz, H., and Sigal, E. (2000) *Arterioscler. Thromb. Vasc. Biol.* **20,** 2100–2105
8. Zhao, L., and Funk, C. D. (2004) *Trends Cardiovasc. Med.* **14,** 191–195
9. Schneider, C., Pratt, D. A., Porter, N. A., and Brash, A. R. (2007) *Chem. Biol.* **14,** 473–488
10. Henriksson, P., Hamberg, M., and Diczfalusy, U. (1985) *Biochim. Biophys. Acta* **834,** 272–274
11. Lin, L., Balazy, M., Pagano, P. J., and Nasjletti, A. (1994) *Circ. Res.* **74,** 197–205
12. Zhu, D., Medhora, M., Campbell, W. B., Spitzbarth, N., Baker, J. E., and Jacobs, E. R. (2003) *Circ. Res.* **92,** 992–1000
13. Hugou, I., Blin, P., Henri, J., Daret, D., and Larrue, J. (1995) *Atherosclerosis* **113,** 189–195
14. Rao, G. N., Baas, A. S., Glasgow, W. C., Eling, T. E., Runge, M. S., and Alexander, R. W. (1994) *J. Biol. Chem.* **269,** 32586–32591
15. Tang, X., Holmes, B. B., Nithipatikom, K., Hillard, C. J., Kuhn, H., and

Campbell, W. B. (2006) *Arterioscler. Thromb. Vasc. Biol.* **26,** 78–84
16. Chava, K. R., Karpurapu, M., Wang, D., Bhanoori, M., Kundumani-Sridharan, V., Zhang, Q., Ichiki, T., Glasgow, W. C., and Rao, G. N. (2009) *Arterioscler. Thromb. Vasc. Biol.* **29,** 809–815
17. Potula, H. S., Wang, D., Quyen, D. V., Singh, N. K., Kundumani-Sridharan, V., Karpurapu, M., Park, E. A., Glasgow, W. C., and Rao, G. N. (2009) *J. Biol. Chem.* **284,** 31142–31155
18. Darnell, J. E., Jr. (1997) *Science* **277,** 1630–1635
19. Hirano, T., Ishihara, K., and Hibi, M. (2000) *Oncogene* **19,** 2548–2556
20. Hou, S. X., Zheng, Z., Chen, X., and Perrimon, N. (2002) *Dev. Cell.* **3,** 765–778
21. Ihle, J. N., and Kerr, I. M. (1995) *Trends Genet.* **11,** 69–74
22. Levine, R. L., and Gilliland, D. G. (2008) *Blood* **112,** 2190–2198
23. Silva, C. M. (2004) *Oncogene* **23,** 8017–8023
24. Yeh, M., Gharavi, N. M., Choi, J., Hsieh, X., Reed, E., Mouillesseaux, K. P., Cole, A. L., Reddy, S. T., and Berliner, J. A. (2004) *J. Biol. Chem.* **279,** 30175–30181
25. Liu, Z., Zhang, C., Dronadula, N., Li, Q., and Rao, G. N. (2005) *J. Biol. Chem.* **280,** 14700–14708
26. Cheranov, S. Y., Karpurapu, M., Wang, D., Zhang, B., Venema, R. C., and Rao, G. N. (2008) *Blood* **111,** 5581–5591
27. Cheranov, S. Y., Wang, D., Kundumani-Sridharan, V., Karpurapu, M., Zhang, Q., Chava, K. R., and Rao, G. N. (2009) *Blood* **113,** 6023–6033
28. Berkner, K. L. (1988) *Biotechniques* **6,** 616–629
29. Dronadula, N., Rizvi, F., Blaskova, E., Li, Q., and Rao, G. N. (2006) *J. Lipid Res.* **47,** 767–777
30. Palomeque, J., Rueda, O. V., Sapia, L., Valverde, C. A., Salas, M., Petroff, M. V., and Mattiazzi, A. (2009) *Circ. Res.* **105,** 1204–1212
31. Wang, D., Liu, Z., Li, Q., Karpurapu, M., Kundumani-Sridharan, V., Cao, H., Dronadula, N., Rizvi, F., Bajpai, A. K., Zhang, C., Müller-Newen, G., Harris, K. W., and Rao, G. N. (2007) *Circ. Res.* **100,** 807–816
32. Bendeck, M. P., Zempo, N., Clowes, A. W., Galardy, R. E., and Reidy, M. A. (1994) *Circ. Res.* **75,** 539–545
33. Gschwind, A., Prenzel, N., and Ullrich, A. (2002) *Cancer Res.* **62,** 6329–6336
34. Samanta, A. K., Lin, H., Sun, T., Kantarjian, H., and Arlinghaus, R. B. (2006) *Cancer Res.* **66,** 6468–6472
35. Liu, Y., Zhao, H., Li, H., Kalyanaraman, B., Nicolosi, A. C., and Gutterman, D. D. (2003) *Circ. Res.* **93,** 573–580
36. Oeckler, R. A., Kaminski, P. M., and Wolin, M. S. (2003) *Circ. Res.* **92,** 23–31
37. Lim, Y. B., Park, T. J., and Lim, I. K. (2008) *J. Biol. Chem.* **283,** 33110–33118
38. Daub, H., Weiss, F. U., Wallasch, C., and Ullrich, A. (1996) *Nature.* **379,** 557–560
39. Fujiyama, S., Matsubara, H., Nozawa, Y., Maruyama, K., Mori, Y., Tsutsumi, Y., Masaki, H., Uchiyama, Y., Koyama, Y., Nose, A., Iba, O., Tateishi, E., Ogata, N., Jyo, N., Higashiyama, S., and Iwasaka, T. (2001) *Circ. Res.* **88,** 22–29
40. Rao, G. N. (1996) *Oncogene* **13,** 713–719
41. Tanimoto, T., Lungu, A. O., and Berk, B. C. (2004) *Circ. Res.* **94,** 1050–1058
42. Yokomizo, T., Kato, K., Hagiya, H., Izumi, T., and Shimizu, T. (2001) *J. Biol. Chem.* **276,** 12454–12459
43. Chaturvedi, P., Reddy, M. V., and Reddy, E. P. (1998) *Oncogene* **16,** 1749–1758
44. Srivastava, K., Kundumani-Sridharan, V., Zhang, B., Bajpai, A. K., and Rao, G. N. (2007) *Cancer Res.* **67,** 4328–4336
45. Wang, D., Paria, B. C., Zhang, Q., Karpurapu, M., Li, Q., Gerthoffer, W. T., Nakaoka, Y., and Rao, G. N. (2009) *Circ. Res.* **104,** 1066–1075
46. Chan, A. K., Kalmes, A., Hawkins, S., Daum, G., and Clowes, A. W. (2003) *J. Vasc. Surg.* **37,** 644–649
47. Seki, Y., Kai, H., Shibata, R., Nagata, T., Yasukawa, H., Yoshimura, A., and Imaizumi, T. (2000) *Circ. Res.* **87,** 12–18
48. Shibata, R., Kai, H., Seki, Y., Kato, S., Wada, Y., Hanakawa, Y., Hashimoto, K., Yoshimura, A., and Imaizumi, T. (2003) *Hum. Gene Ther.* **14,** 601–610
49. Kovacic, J. C., Gupta, R., Lee, A. C., Ma, M., Fang, F., Tolbert, C. N., Walts, A. D., Beltran, L. E., San, H., Chen, G., St Hilaire, C., and Boehm, M. (2010) *J. Clin. Invest.* **120,** 303–314
50. Schwaiberger, A. V., Heiss, E. H., Cabaravdic, M., Oberan, T., Zaujec, J., Schachner, D., Uhrin, P., Atanasov, A. G., Breuss, J. M., Binder, B. R., and Dirsch, V. M. (2010) *Arterioscler. Thromb. Vasc. Biol.* **30,** 2475–2481